γ-Fe_2O_3 Nanoparticles Covered with Glutathione-Modified Quantum Dots as a Fluorescent Nanotransporter

Zbynek Heger, Natalia Cernei, Iva Blazkova, Pavel Kopel, Michal Masarik, Ondrej Zitka, Vojtech Adam & Rene Kizek

Chromatographia
An International Journal for Rapid Communication in Chromatography, Electrophoresis and Associated Techniques

ISSN 0009-5893
Volume 77
Combined 21-22

Chromatographia (2014) 77:1415-1423
DOI 10.1007/s10337-014-2732-7

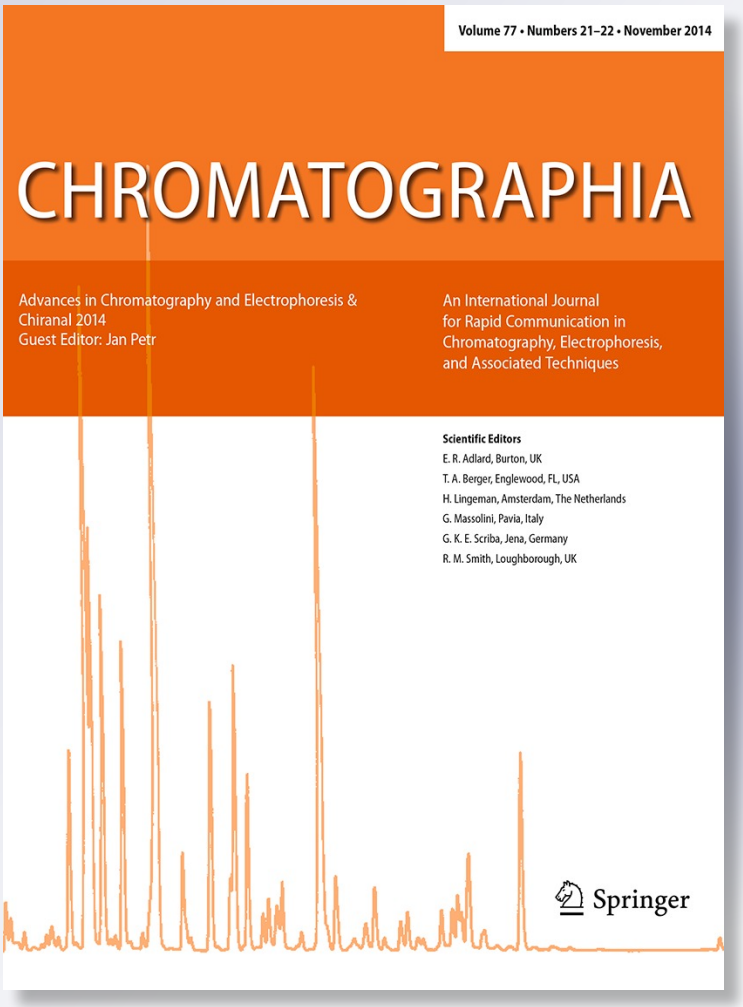

Springer

Chromatographia (2014) 77:1415–1423
DOI 10.1007/s10337-014-2732-7

ORIGINAL

γ-Fe_2O_3 Nanoparticles Covered with Glutathione-Modified Quantum Dots as a Fluorescent Nanotransporter

Zbynek Heger · Natalia Cernei · Iva Blazkova · Pavel Kopel · Michal Masarik · Ondrej Zitka · Vojtech Adam · Rene Kizek

Received: 12 February 2014 / Revised: 22 June 2014 / Accepted: 25 June 2014 / Published online: 17 August 2014

Abstract The present paper describes the synthesis, characterization, and utilization of multi-functional magnetic conjugates that integrate optical and magnetic properties in a single structure for use in many biomedical applications. Spontaneous interaction with eukaryotic cell membrane (HEK-239 cell culture) was determined using fluorescence microscopy, and fluorescence analyses. Both, differences in excitation, and emission wavelength were observed, caused by glutathione intake by cells, resulting in disintegration of core–shell structure of quantum dots, as well as adhesion of conjugate onto cell surface. When compared with quantum dots fluorescent properties, HEK-239 cells with incorporated nanoconjugate exhibited two excitation maxima (λ_{ex} = 430 and 390 nm). Simultaneously, application of ideal λ_{ex} for quantum dots (λ_{ex} = 430 nm), resulted in two emission maxima (λ = 740 and 750 nm). This nanoconjugate fulfills the requirements of term theranostics, because it can be further functionalized with biomolecules as DNA, proteins, peptides or antibodies, and thus serves as a tool for therapy in combination with simultaneous treatment.

Keywords Excitation · HEK-239 · Luminescence · Nanoconjugate · Theranostics

Published in the topical collection *Advances in Chromatography and Electrophoresis & Chiranal 2014* with guest editor Jan Petr.

Z. Heger · N. Cernei · I. Blazkova · P. Kopel · O. Zitka · V. Adam · R. Kizek (✉)
Department of Chemistry and Biochemistry, Faculty of Agronomy, Mendel University in Brno, Zemedelska 1, 613 00 Brno, Czech Republic
e-mail: kizek@sci.muni.cz

N. Cernei · I. Blazkova · P. Kopel · M. Masarik · O. Zitka · V. Adam · R. Kizek
Central European Institute of Technology, Brno University of Technology, Technicka 3058/10, 616 00 Brno, Czech Republic

M. Masarik
Department of Pathological Physiology, Faculty of Medicine, Masaryk University, Kamenice 5, 625 00 Brno, Czech Republic

Introduction

Over the past decade, magnetism and magnets have found a growing field of application in the areas of biotechnology and medical technology. Combining the forces of magnetism with micro- and nanotechnology has further miniaturized the modes of application [1]. Examples of applications range from magnetoresistive-based biosensors, visualization of common biological events, to nanomedicine [2–4].

Maghemite (γ-Fe_2O_3) is iron oxide, able to form particles smaller than 10 nm showing superparamagnetic and paramagnetic properties at room temperature [5]. The possibilities of iron oxide nanoparticles have markedly increased due to the versatile characteristics of these materials arising from the ability to manipulate and control their surface functionalities, and thus to form potentially novel material with wide range of applications. One big advantage of iron oxide nanoparticles is their biocompatibility and low toxicity vertebrates [6, 7], predestining nanomaghemite to enhance the theranostic possibilities. Within the medical field, nanomaghemite has been studied widely to enhance cancer treatment, and diagnostic techniques, such as drug delivery systems [8–10], photoabsorbers in photodynamic therapies [11, 12], hyperthermia in cancer therapies [13–15], and magnetic resonance imaging (MRI) contrast agent carriers [16–18].

Nanoparticles like maghemite, as well as carbon nanotubes, and others lack fluorescent properties sufficient to

monitor their optical transport in vitro or in vivo, limiting the study of their transport [19]. Even though gadolinium has been used to enhance contrast of iron oxide nanoparticles by Kim and colleagues, and they demonstrated the potential of iron oxide nanoparticles as T_1 MRI contrast agents in clinical settings [20], only few attempts have been made to optically track nanomaghemite interaction in eukaryotic cells [21, 22].

Employment of quantum dots as labels offers numerous advantages, as they are resistant to both photo- and chemical degradation over time, and they provide a wide excitation band with a narrow emission band [23]. Furthermore they exhibit pronounced brightness compared to other fluorophores. A lot of studies have been aimed at determination of both in vitro and in vivo toxicity of these nanoparticles and the results are promising to use these nanomaterials in vivo. It was shown that QDs toxicity is highly dependent on QDs crystal size, stability in solution, as well as physical environment [24–26]; however, the use of properly prepared and modified QDs had negligible toxicity. Moreover, these particles can be conjugated to other materials as they were successfully conjugated to maghemite nanoparticles through covalent binding [27], or using binders like 3-aminopropyltrimethoxysilane (APTES) [28]. Generally, in core–shell QDs such as ZnSe/CdS or CdTe/CdS the shell material is grown onto the core material to reduce the nonradiative recombination effectively by confining the wave function of an electron–hole pair to the interior of core material [29, 30]. Such core–shell particles display efficient luminescence with stability superior to single phase nanoparticles and organic dyes and are of great interest for biological imaging and light-emitting devices [31].

The aim of this study was preparation of conjugate comprising CdTe/CdS quantum dots (QDs) with nanomaghemite and application of the human embryonic kidney 293 cell culture (HEK-293). We hypothesized that GSH stabilization of QDs may provide interaction with cell membranes. Moreover, the adsorption of cells on surface of conjugate can be utilized for separation of cells from medium.

Experimental Section

Chemicals

Standards and other chemicals were purchased from Sigma-Aldrich (St. Louis, MO, USA) in ACS purity, unless noted otherwise. Working solutions like buffers and standard solutions were prepared daily by diluting the stock solutions with deionized water obtained by using reverse osmosis equipment Aqual 25 (Aqual s.r.o., Brno, Czech Republic). The deionized water was further purified by using an apparatus Direct-Q 3 UV Water Purification System equipped with an UV lamp (Millipore, Billerica, MA, USA). The resistance was established to 18 MΩ cm^{-1}. The pH was measured using a pH meter WTW inoLab (Weilheim, Germany).

Cell Culture

The HEK-293 cells were cultured in Dulbecco's modified Eagle's medium (DMEM) supplemented with 10 % foetal bovine serum (FBS, Gibco, Grand Island, NY, USA), 2 mM L-glutamine, 100 U mL^{-1} of penicillin, and 100 μg mL^{-1} of streptomycin in a humidified chamber at 37 °C and 5 % CO_2. Selected cells were subjected to in vitro interaction with 10 μL of GSH-QDs@nanomaghemite in concentration of 500 μg mL^{-1} prepared in the presence of phosphate-buffered saline (PBS).

Synthesis of Nanoparticles

Nanomaghemite particles were prepared according to the following protocol: Briefly, 5 g of $FeCl_3 \cdot 6H_2O$ was dissolved in 400 mL of water and subsequently 1 g of $NaBH_4$ in 50 mL of 3.5 % NH_3 [7 mL 25 % NH_3 in 43 mL of H_2O (v/v)] was added. Mixture was heated for 2 h at 100 °C. After cooling to room temperature, nanomaghemite was separated using the magnetic force of external magnetic field. Further, maghemite nanoparticles were washed five times with water and dried at 40 °C.

CdTe/CdS quantum dots were prepared as follows: (I) solution of CdTe QDs was prepared by dissolving the cadmium acetate dihydrate (0.044 g) in 76 mL of MiliQ water using the stirrer Biosan OS-10 (Biosan, Riga, Latvia). Further, 60 mg of mercaptosuccinic acid (MSA) dissolved in 1 mL of water was added followed by addition of 1.8 mL of 1 M NH_3. Finally, solution of Na_2TeO_3 (0.0055 g) was added and after few minutes 50 mg of $NaBH_4$ was poured into the stirred solution. After 1 h lasting stirring, volume was adjusted to 100 mL using water and further, the solution was heated in microwave reactor Multiwave 300 (Anton Paar, Graz, Austria) using conditions as follows: 300 W, 120 °C, 10 min. (II) solution of CdS was prepared using a reaction of cadmium acetate dihydrate (0.022 g) with reduced glutathione (0.1229 g) and 1 mL of 1 M NH_3 in 24 mL of water. Further, sodium sulphate nonhydrate (0.012 g) in water (25 mL) was added under stirring, lasting 2 h. (III) finally CdTe/CdS QDs were prepared by mixing of 1 mL of both solutions together in glass vial subsequently heated in microwave reactor at 90 °C for 10 min (Multiwave 300, Anton Paar, Graz, Austria).

GC Organic Elemental Analysis

To obtain the basic information about QDs organic element composition, liquid sample of QDs was dried at 220 °C,

and analysed using Automatic elemental analyzer Flash 2000 (Thermo Fisher Scientific, Waltham, MA, USA), equipped with two isothermal GC separation columns (CHN/NC separation columns, 2 m, 6 × 5 mm Stainless, PQS, 2 mm unions, OEA Laboratories Limited, Callington, UK) and thermal conductivity detector (TCD). The flow rate of helium was set to 140 mL min^{-1}, and the separation temperature was set to 65 °C.

Fluorescence Measurements

X-ray fluorescence element analysis was carried out on Xepos (SPECTRO analytical instruments GmbH, Kleve, Germany) fitted with three detectors: Barkla scatter—aluminium oxide, Barkla scatter—HOPG and Compton/secondary molybdenum respectively. Analyses were conducted in Turbo Quant cuvette method of measurement. The parameters for analysis were as follows—measurement duration: 300 s, tube voltage from 24.81 to 47.72 kV, tube current from 0.55 to 1.0 mA, with zero peak at 5,000 cps and vacuum switched off. Fluorescence analyses were carried out on multifunctional microplate reader Tecan Infinite 200 PRO (TECAN, Maennedorf, Switzerland). Sample was applied into UV-transparent 96 well microplate with flat bottom Costar® purchased from Corning Inc. (NY, USA). The dose per well was 50 μL of sample for all analysed variants. All measurements were performed at 30 °C controlled by Tecan Infinite 200 PRO (TECAN, Switzerland). For the fluorescence measurements of QDs, excitation wavelength was set to $\lambda_{ex} = 430$ nm, and the fluorescence scans were carried out within the range from 500 to 870 nm (emission wavelength step size: 5 nm, gain: 90; number of flashes: 5).

UV/VIS Spectrophotometry

Absorbance analyses were carried out using UV/VIS spectrophotometer SPECORD 210 (Analytik Jena, Jena, Germany). Carousel was tempered to 37 °C by a flow thermostat Julabo F25 (Julabo, Seelbach, Germany), with volume of sample 200 μL per analysis.

Ion-Exchange Liquid Chromatography

For identification of glutathione presence in the synthesized quantum dots, the ion-exchange liquid chromatography with post column derivatization by ninhydrin and the absorbance detector operating in the VIS range at 440 nm was employed. Glass column tempered to 60 °C with inner diameter of 3.7 mm and 350 mm length was filled manually with strong cation exchanger in sodium cycle LG ANB with approximately 12 μm particles and 8 % porosity. The elution mobile phase (pH 2.7) contained 11.11 g of citric acid, 4.04 g of sodium citrate, 9.25 g of NaCl, 0.1 g of sodium azide and 2.5 mL of thiodyglycol per liter of solution, using the flow rate of 0.25 mL min^{-1}. Other experimental conditions were used as previously published [32].

Microscopy

Microscopic studies were performed using an inverted Olympus IX 71S8F-3 fluorescence microscope (Olympus, Tokyo, Japan) equipped with a mercury arc lamp HBO 50 W (OSRAM GmbH, Munich, Germany) for illumination. The excitation filter 545–580 nm and the emission filter of 610 nm was employed. Images were acquired with a Camera Olympus DP73 and processed by Stream Basic 1.7 software with the software resolution of 1,600 × 1,200 pixels.

Descriptive Statistics

Mathematical analysis of the data and their graphical interpretation were made using Microsoft Excel®, Microsoft Word® and Microsoft PowerPoint®. Results are expressed as mean ± standard deviation (SD) unless noted otherwise.

Results and Discussion

Characterization of Nanomaghemite@QDs Conjugate

To demonstrate the fluorescence properties of CdTe/CdS quantum dots prepared by us and their conjugate with nanomaghemite, we firstly prepared conjugate comprising QDs@nanomaghemite. As it was described previously by Chowdhury et al. [33], iron oxide nanoparticles adsorption towards cadmium proceeds very willingly. In their adsorption study, using mixture of maghemite and magnetite it was shown that cadmium may become fixed by complexation with oxygen atoms in the oxy-hydroxy groups at the shell surface of the iron oxide nanoparticles. Moreover, the coupling between the CdTe/Cds QDs and the nanometric iron oxide particles was supported by thiol chemistry. Thiols (–SH) are probably the mostly utilized functional groups for modifying the QDs, due to thiol groups natural ability to bind with metals on the surface of QDs [34–36]. Therefore we decided to use self-assembly adsorption of 1 mL of QDs onto 2 mg of nanomaghemite, and after 5 min lasting interaction, remaining liquid was removed using external magnetic field. This procedure was made once and then conjugate was resuspended with 2 mL of phosphate buffered saline (PBS).

Figure 1 shows the photographs of the CdTe/CdS@nanomaghemite solution after 5 min lasting interaction (Fig. 1a), CdTe/CdS (Fig. 1b), and the solution

of nanomaghemite in PBS without QDs (Fig. 1c). QDs exhibited a homogenous physical state, until binding to nanomaghemite was established (Fig. 1a). Although maghemite nanoparticles quickly sink to the bottom, they should be rapidly dispersed using a force of external magnetic field, due to their excellent paramagnetic properties [37–40]. When excited under UV lamp (λ_{ex} = 312 nm), as it is shown in Fig. 1aa–ca, both the solution of CdTe/Cds@nanomaghemite (10 min stirred for perfect dispersion of nanoparticles), and CdTe/Cds exhibited red–orange emission, caused by the uniformity in particle size as a result of the quantum-confinement effect [41].

To obtain more information about elemental characteristics of glutathione-modified CdTe/CdS quantum dots, X-ray fluorescence (XRF), and gas chromatography with TCD were employed. As it is shown in Fig. 2a, expressing percentual representation of elements forming QDs, the most abundant element was sulphur, represented with 21.25 %. Sulphur was primarily used for synthesis of CdS as a part of CdTe/CdS QDs. Moreover, sulphur is contained in glutathione comprising thiol groups as the most utilized ligands for stabilization of semiconductors and noble metal nanocrystals [31, 42]. Cadmium was identified as second in row, in the manner of quantity with 19.49 % from total elemental composition, as it was used as a main element in QDs synthesis. Finally tellurium was determined as plentiful in QDs sample with 7.8 %. Although sulphur was determined as the most abundant element using X-ray fluorescence, this method is limited in sense of detection of organic elements. Hence, to obtain further insight into QDs organic elemental composition the GC-TCD was employed (Fig. 2a). Interestingly it was found that even though the sulphur amount, determined using XRF was approximately comparable with other determined elements, using GC-TCD; sulphur was shown to form only a small amount of organic elements portion when compared to nitrogen, hydrogen and carbon. This phenomenon aims at large amount of glutathione, covering the surface of quantum

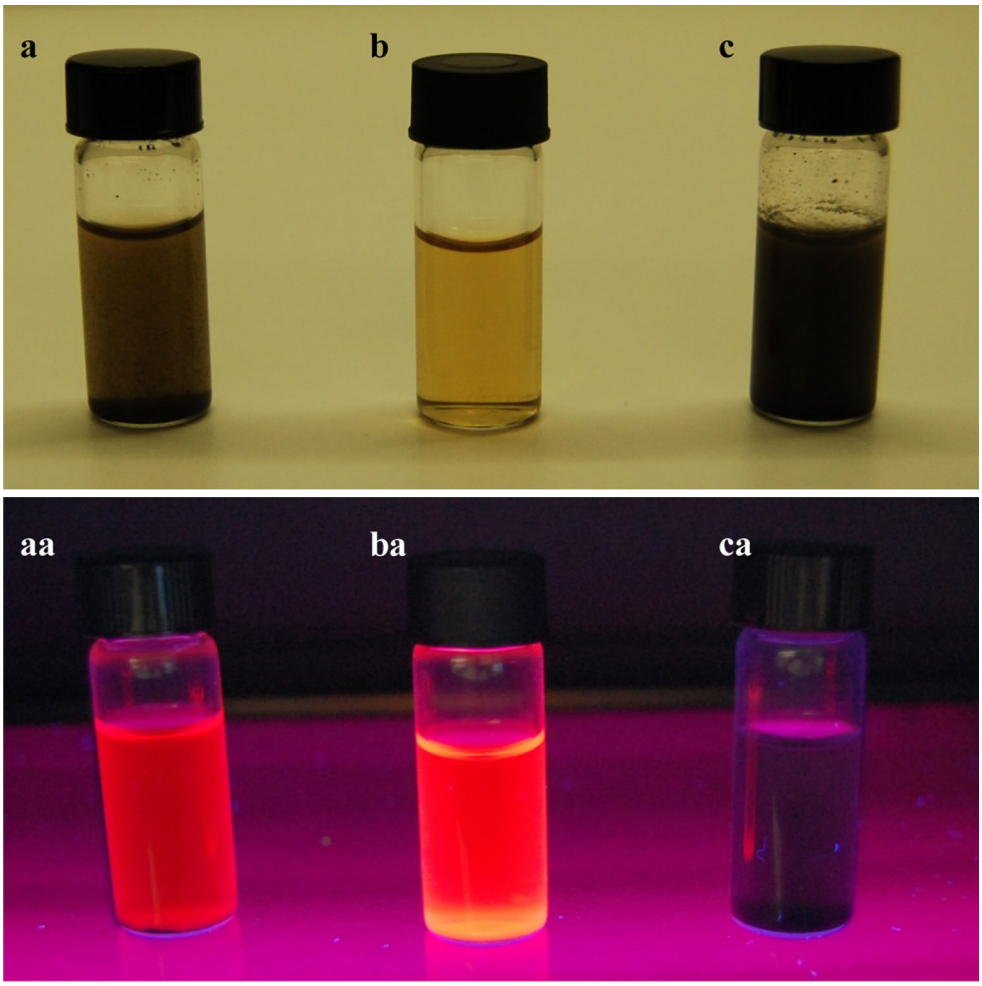

Fig. 1 Photography of quantum dots **a** bound on nanomaghemite nanoparticles, **b** without nanoparticles binding, **c** of nanoparticles dispersion without QDs. With down case letters (**a, b, c**) there are shown pictures of the same solutions under the UV light (λ_{ex} = 312 nm)

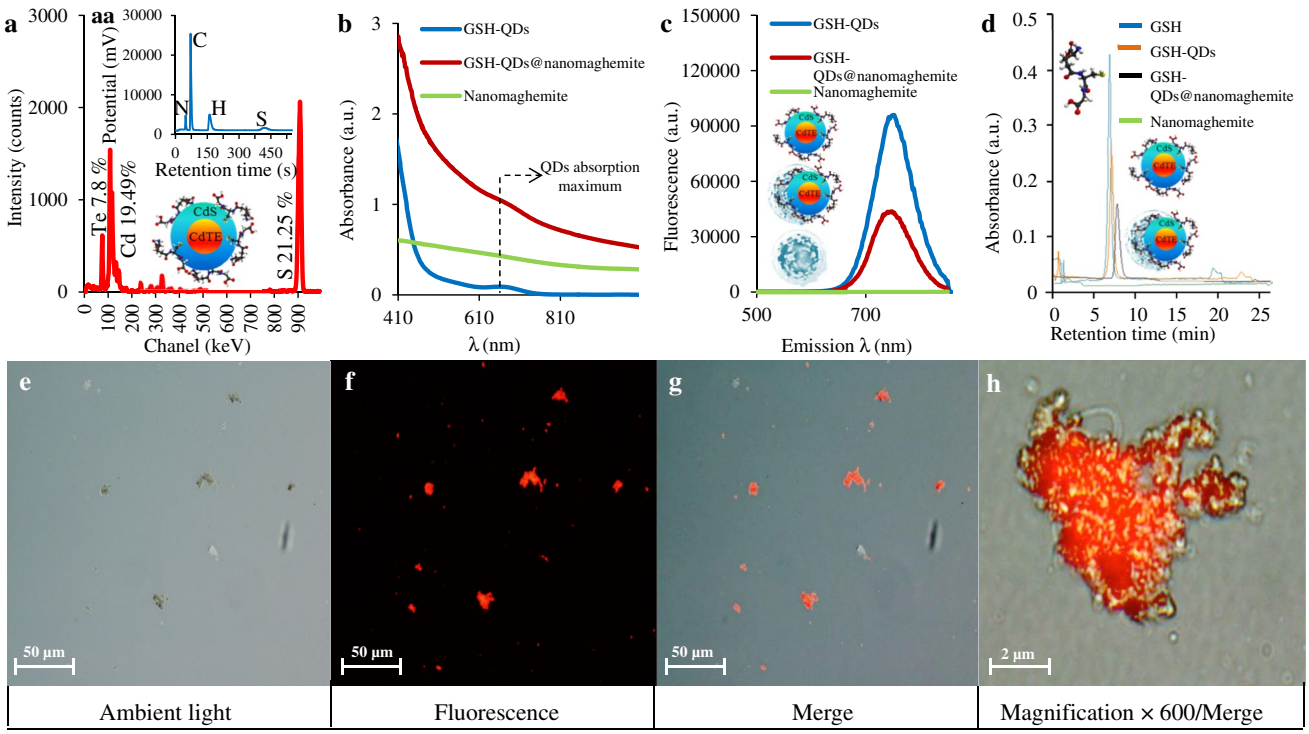

Fig. 2 Characterization of GSH-stabilized CdTe/CdS core–shell quantum dots (hereinafter GSH-QDs). **a** X-ray fluorescence expression of elemental composition of our semiconductor nanocrystals with (*aa*) showing gas chromatographic (GC-TCD) results. **b** Absorbance of GSH-QDs and absorbance of complex after binding on nanomaghemite (hereinafter GSH-QDs@nanomaghemite). **c** The expression of fluorescence of GSH-QDs and GSH-QDs@nanomaghemite with detector gain set to 90, and excitation ($\lambda_{ex} = 430$ nm). **d** The presence of glutathione in GSH-QDs complex determined using ion-exchange chromatography with postcolumn derivatization with ninhydrin, and subsequent VIS detection ($\lambda = 440$ nm). **e** Microphotograph of GSH-QDs@nanomaghemite **f** as well as fluorescence microphotograph; and **g** merging of these two images. The particles were photographed under a microscope using magnification × 100. **h** Microphotograph (merged) of GSH-QDs@nanomaghemite using magnification × 600

dots, making the nanoparticles more stable, and accessible for interaction with other molecules.

It is shown in Fig. 2b that absorbance of both QDs and QDs@nanomaghemite conjugate shows the same maximum at approximately $\lambda = 660$ nm, pointing at red colour of QDs. The elevation in absorbance values of QDs@nanomaghemite conjugate is caused by the presence of maghemite nanoparticles, causing the measured solution turbid, and thus more immersive for spectrophotometer´s beam. Hence, the absorption maximum of QDs@nanomaghemite is shifted slightly to the right in the VIS region. Fluorescence measurements of QDs and QDs@nanomaghemite conjugate, according to emission maxima, show that the fluorescence behaviour of CdTe/CdS after binding with nanomaghemite was retained, but the emission yield was decreased, due to binding, and thus partial quenched (Fig. 2c). Quenching may be caused due to several reasons, like non-radiative transfer on the surface of the particle, leading to a strong absorption of the transmitted light by the iron oxide nanoparticles, as it was described by Dubertret et al. [43], or due to a close presence of individual fluorophores, causing inter-molecule quenching [44]. Despite the quenching of luminescent QDs, quantum yields are still sufficient for labelling applications.

Because elemental analysis showed relatively large portion of organic elements, probably originated from glutathione, we carried out ion-exchange liquid chromatography (IELC) analysis to gain further insight into glutathione portion in quantum dots (Fig. 2d). Both QDs and QDs@nanomaghemite conjugate were dissolved in 3 M HCl prior to LC analysis, and subsequently evaporated using nitrogen blow-down evaporator Ultravap 96 with spiral needles (Porvair Sciences Limited, Leatherhead, UK), following protocol commonly used by us for LC analyses of various analytes bound on paramagnetic particles [32, 45]. According to calibration curve, carried out for glutathione ($y = 0.2985x + 0.695$, $R^2 = 0.9965$), amount of peptide in CdTe/CdS quantum dots was determined as 13 µg mL^{-1} of QDs solution, and glutathione retained very similar retention time (7.11 min) when compared with standard in concentration of 30 µg mL^{-1} (7.25 min). GSH content in QDs@nanomaghemite conjugate was evaluated to 9 µg mL^{-1}, and retention time of peptide was slightly

shifted (8.09 min). The shift can be related to the interactions of GSH covered QD with nanomaghemite. Lower portion of glutathione was caused by recovery of nanoparticles that may be calculated as $GSH_{QDs@nanomaghemite}/GSH_{QDs} \times 100$, and was found as 69 %. Recovery in this manner was caused by partial clustering of nanometric maghemite particles that were shown to cluster willingly in powder form [46], and thus reduce their functional surface.

As it was mentioned above, although quenching, and clustering phenomenons were observed, QDs@nanomaghemite conjugate was still very simple detectable using fluorescence microscopy (Figs. 2e–h), exhibiting red–orange emission, using QD fluorescence filter which operates in $\lambda_{ex} = 430$–475 nm (Nikon, Tokyo, Japan).

Cell Experiment

To demonstrate further the practical application of QDs@nanomaghemite conjugate, we carried out experiment with HEK-239 cells (Fig. 3). The obtained results revealed that conjugate can be used as a fluorescent and magnetic forced tool for distribution of therapeutics targeted to membrane organelles of cells. It was shown that after >30 min lasting interactions, the prepared conjugate adhered onto cells surface, as it is distinctly indicated in Fig. 3a–cb, using magnification ×400. This effect is caused by high absorption capability of maghemite nanoparticles, as well as by modification of glutathione providing NH_2; –COOH or –SH moieties' that can be possible available for

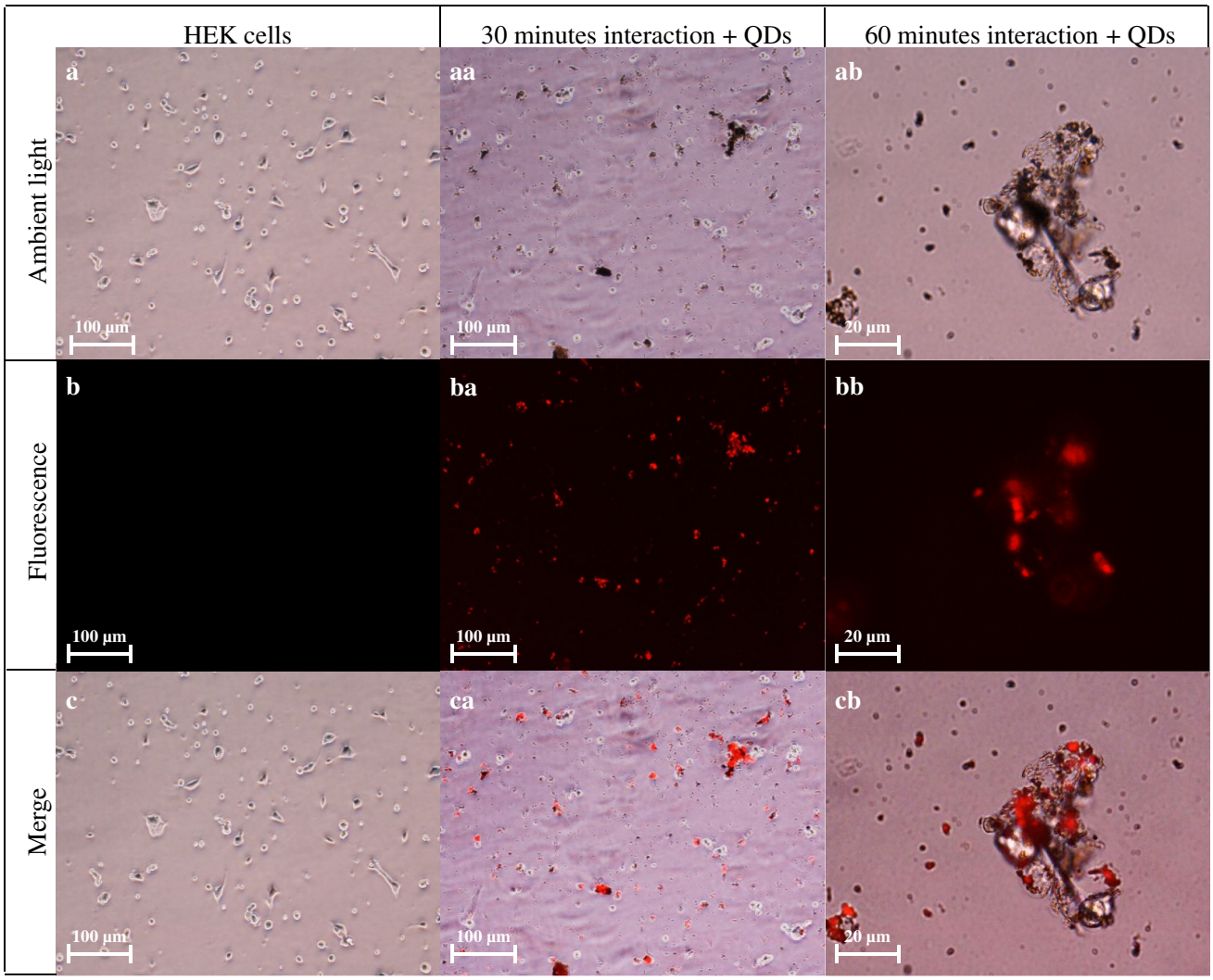

Fig. 3 Microphotographs of **a** HEK-239 cells in ambient light; **b** their fluorescence; and **c** merged ambient light with fluorescence. As a *downcase letter* there are highlighted microphotographs of HEK-239 cells **a** after 30 min lasting interaction with GSH-QDs@nanomaghemite, **b** after 1 h lasting interaction with GSH-QDs@nanomaghemite, and **c** merged ones. The cells were photographed under a microscope (×100; and ×400 respectively in the case of **a**–**cb**). Interactions were performed at 37 °C under a humidified atmosphere containing 5 % CO_2

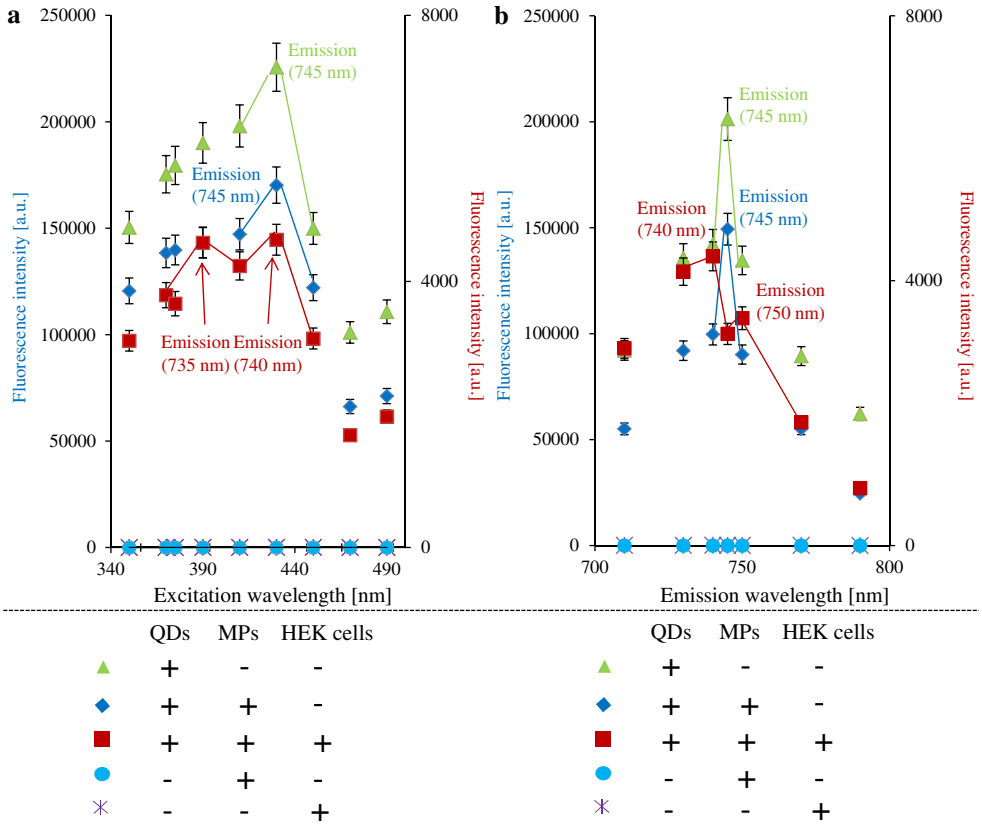

Fig. 4 **a** Expression of excitation scans (excitation λ_{ex} = 350–490 nm) carried out for all individual parts of complex as well as for HEK-239 cells. There are emission maxima for the ideal excitation wavelengths, showing different fluorescent behaviour of complex adhered on a surface of the HEK cells (*red square*). **b** Expression of emission scans, using ideal excitation obtained from previous measurement (λ_{ex} = 430 nm). Two peaks of emission maxima were observed after adhesion of complex on a surface of the HEK cells (*red square*). Detector gain for both analyses was set to 100

interaction [47, 48], but the mostly utilized binding moiety has to be further examined. Cells intake of glutathione is rapidly increasing during various pathological conditions, as oxidative stress, nitrosative stress, inflammatory, cancer, chemotherapy, ionizing radiation, heat shock, heavy metals intake and many others [49–51], and thus conjugate may serve as a targeted nanotransporter, as well as a diagnostic tool, meeting the conditions of theranostics term. Moreover, conjugate also offers many possibilities to be functionalized with biomolecules as DNA, proteins, peptides, or antibodies. There is also important to mention that this system can be utilized as bimodal anticancer agents for combined chemotherapeutic and hyperthermia and/or photodynamic therapy [52, 53].

Besides basic microscopy, fluorescence analyses were performed to obtain information about cells influence on quantum dots excitation, and emission yields. Prior to fluorescence analyses, HEK-239 cells were divided of DMEM, after interaction with QDs@nanomaghemite using external magnetic field for their separation from medium and intriguingly, the bond between conjugate and cells was strong enough to withstand three washing steps with PBS. Further cells were resuspended with PBS to final volume of 50 μL in 96-well microplate with flat bottom Costar® purchased by Corning (NY, USA). Primarily, we carried out excitation scan analysis (Fig. 4a). Interestingly, when compared with QDs and QDs@nanomaghemite, in HEK-239 cells, after interaction, there were determined two excitation maxima at cell culture. First one, identical with excitation of QDs (λ_{ex} = 430 nm), but with different emission maximum (λ = 740 nm for HEK-239 cells, compared with 745 nm for QDs), and second one at 390 nm with emission maximum of 735 nm. This phenomenon points at interaction elapsed on the cell membranes, likely influenced by degradation of glutathione from the surface of QDs@nanomaghemite conjugate, causing partial disintegration of CdS shell from CdTe core. Hence, the fluorescence properties of QDs composite are changed. Similar results were observed using ideal excitation, obtained from previous analysis (λ_{ex} = 430 nm), to obtain emission maxima scans (Fig. 4b). Expected emission maximum of cell culture (740 nm) was observed, but second maximum was

determined also at emission wavelength of 750 nm. This maximum exhibited lower fluorescence value, but again pointed at changed luminescence properties of the prepared conjugate, after interaction with cell membrane. These data may serve as evidence that QDs@nanomaghemite conjugate spontaneously interact with eukaryotic cell membrane, and thus has a potential to offer many biomedical possibilities, such as nanotransporters into tumorous cells, where increased oxidative stress commonly occurs.

Conclusions

In our study, we showed that water dispersible, multi-functional CdTe/CdS quantum dots, stabilized with glutathione may be utilized for labelling of maghemite nanoparticles, and thus they can offer the possibility to observe the interactions between iron oxide nanometric particles and eukaryotic cells (HEK-239 in this case). Moreover, the resulting conjugate QDs@nanomaghemite demonstrated excellent fluorescent and paramagnetic properties. We revealed the possibility of QDs@nanomaghemite to serve as a labelled nanotransporter of drugs, targeted to the molecular structures, placed on cell membranes. Approach in this manner may fulfil the requirements of theranostics term, because it can be further functionalized with biomolecules as DNA, proteins, peptides or antibodies, and thus serve as a tool for therapy in combination with simultaneous treatment. Moreover, the presence of iron nanoparticles provides the possibility of application in hyperthermic, and/or photodynamic therapy. Functionalization of magnetically doped QDs with Gd^{3+} ions may show potential also as a MR contrast agent, too.

Acknowledgments The authors are grateful to CEITEC CZ.1.05/1.1.00/02.0068 for financial support. The authors also with to express their thanks to Lukas Melichar for perfect technical assistance.

Conflict of interest The authors have declared no conflict of interest.

References

1. Pamme N (2006) Lab Chip 6:24–38
2. Graham DL, Ferreira HA, Freitas PP (2004) Trends Biotechnol 22:455–462
3. Miller MM, Sheehan PE, Edelstein RL, Tamanaha CR, Zhong L, Bounnak S, Whitman LJ, Colton RJ (2001) J Magn Magn Mater 225:138–144
4. Skaat H, Shafir G, Margel S (2011) J Nanopart Res 13:3521–3534
5. Teja AS, Koh PY (2009) Prog Cryst Growth Charact Mater 55:22–45
6. Majewski P, Thierry B (2007) Crit Rev Solid State Mat Sci 32:203–215
7. Kim JS, Yoon TJ, Kim BG, Park SJ, Kim HW, Lee KH, Park SB, Lee JK, Cho MH (2006) Toxicol Sci 89:338–347
8. Silva AKA, Silva EL, Carrico AS, Egito EST (2007) Curr Pharm Design 13:1179–1185
9. Neuberger T, Schopf B, Hofmann H, Hofmann M, von Rechenberg B (2005) J Magn Magn Mater 293:483–496
10. Lubbe AS, Bergemann C, Riess H, Schriever F, Reichardt P, Possinger K, Matthias M, Dorken B, Herrmann F, Gurtler R, Hohenberger P, Haas N, Sohr R, Sander B, Lemke AJ, Ohlendorf D, Huhnt W, Huhn D (1996) Cancer Res 56:4686–4693
11. Wang C, Cheng L, Liu Z (2013) Theranostics 3:317–330
12. Wang ST, Chen KJ, Wu TH, Wang H, Lin WY, Ohashi M, Chiou PY, Tseng HR (2010) Angew Chem Int Edit 49:3777–3781
13. Valero E, Tambalo S, Marzola P, Ortega-Munoz M, Lopez-Jaramillo FJ, Santoyo-Gonzalez F, Lopez JD, Delgado JJ, Calvino JJ, Cuesta R, Dominguez-Vera JM, Galvez N (2011) J Am Chem Soc 133:4889–4895
14. Meffre A, Mehdaoui B, Kelsen V, Fazzini PF, Carrey J, Lachaize S, Respaud M, Chaudret B (2012) Nano Lett 12:4722–4728
15. Hilger I (2013) Int J Hyperthermia 29:828–834
16. Kaufner L, Cartier R, Wustneck R, Fichtner I, Pietschmann S, Bruhn H, Schutt D, Thunemann AF, Pison U (2007) Nanotechnology 18:1–5
17. Thunemann AF, Schutt D, Kaufner L, Pison U, Mohwald H (2006) Langmuir 22:2351–2357
18. Oghabian MA, Jeddi-Tehrani M, Zolfaghari A, Shamsipour F, Khoei S, Amanpour S (2011) J Nanosci Nanotechnol 11:5340–5344
19. Miyawaki J, Yudasaka M, Imai H, Yorimitsu H, Isobe H, Nakamura E, Iijima S (2006) Adv Mater 18:1010–1014
20. Kim BH, Lee N, Kim H, An K, Park YI, Choi Y, Shin K, Lee Y, Kwon SG, Na HB, Park JG, Ahn TY, Kim YW, Moon WK, Choi SH, Hyeon T (2011) J Am Chem Soc 133:12624–12631
21. Shi SF, Jia JF, Guo XK, Zhao YP, Liu BY, Chen DS, Guo YY, Zhang XL (2012) J Nanopart Res 14:1–11
22. Wilkinson K, Ekstrand-Hammarstrom B, Ahlinder L, Guldevall K, Pazik R, Kepinski L, Kvashnina KO, Butorin SM, Brismar H, Onfelt B, Osterlund L, Seisenbaeva GA, Kessler VG (2012) Nanoscale 4:7383–7393
23. Drbohlavova J, Adam V, Kizek R, Hubalek J (2009) Int J Mol Sci 10:656–673
24. Derfus AM, Chan WCW, Bhatia SN (2004) Nano Lett 4:11–18
25. Gao XH, Cui YY, Levenson RM, Chung LWK, Nie SM (2004) Nat Biotechnol 22:969–976
26. Geys J, Nemmar A, Verbeken E, Smolders E, Ratoi M, Hoylaerts MF, Nemery B, Hoet PHM (2008) Environ Health Perspect 116:1607–1613
27. Wang DS, He JB, Rosenzweig N, Rosenzweig Z (2004) Nano Lett 4:409–413
28. Liu B, Xie WX, Wang DP, Huang WH, Yu MJ, Yao AH (2008) Mater Lett 62:3014–3017
29. Gu ZY, Zou L, Fang Z, Zhu WH, Zhong XH (2008) Nanotechnology 19:1–12
30. Peng H, Zhang LJ, Soeller C, Travas-Sejdic J (2007) J Lumines 127:721–726
31. Chan WCW, Nie SM (1998) Science 281:2016–2018
32. Zitka O, Cernei N, Heger Z, Matousek M, Kopel P, Kynicky J, Masarik M, Kizek R, Adam V (2013) Electrophoresis 34:2639–2647
33. Chowdhury SR, Yanful EK (2013) J Environ Manage 129:642–651
34. Gerion D, Pinaud F, Williams SC, Parak WJ, Zanchet D, Weiss S, Alivisatos AP (2001) J Phys Chem B 105:8861–8871
35. Wuister SF, Swart I, van Driel F, Hickey SG, Donega CD (2003) Nano Lett 3:503–507
36. Aldana J, Wang YA, Peng XG (2001) J Am Chem Soc 123:8844–8850

37. Magro M, Sinigaglia G, Nodari L, Tucek J, Polakova K, Marusak Z, Cardillo S, Salviulo G, Russo U, Stevanato R, Zboril R, Vianello F (2012) Acta Biomater 8:2068–2076
38. Lukashova NV, Savchenko AG, Yagodkin YD, Muradova AG, Yurtov EV (2014) J Alloy Compd 586:S298–S300
39. Rudzka K, Viota JL, Munoz-Gamez JA, Carazo A, Ruiz-Extremera A, Delgado AV (2013) Colloid Surf B-Biointerfaces 111:88–96
40. Giakisikli G, Anthemidis AN (2013) Talanta 110:229–235
41. Salgueirino-Maceira V, Correa-Duarte MA, Spasova M, Liz-Marzan LM, Farle M (2006) Adv Funct Mater 16:509–514
42. Bruchez M, Moronne M, Gin P, Weiss S, Alivisatos AP (1998) Science 281:2013–2016
43. Dubertret B, Calame M, Libchaber AJ (2001) Nat Biotechnol 19:365–370
44. Perez JM, O'Loughin T, Simeone FJ, Weissleder R, Josephson L (2002) J Am Chem Soc 124:2856–2857
45. Zitka O, Heger Z, Kominkova M, Skalickova S, Krizkova S, Adam V, Kizek R (2014) J Sep Sci 37:465–575
46. Hergt R, Dutz S, Muller R, Zeisberger M (2006) J Phys Condes Matter 18:S2919–S2934
47. Yang CY, Huang LY, Shen TL, Yeh JA (2010) Eur Cells Mater 20:415–430
48. Zhang WX, Tong L, Yang C (2012) Nano Lett 12:1002–1006
49. Townsend DM, Tew KD, Tapiero H (2003) Biomed Pharmacother 57:145–155
50. Lu SC (2000) Curr Top Cell Reg 36:95–116
51. Kinter M, Roberts RJ (1996) Free Radic Biol Med 21:457–462
52. Gu HW, Xu KM, Yang ZM, Chang CK, Xu B (2005) Chem Commun 2005:4270–4272
53. Zebli B, Susha AS, Sukhorukov GB, Rogach AL, Parak WJ (2005) Langmuir 21:4262–4265